Solid State Communications 318 (2020) 113963

Contents lists available at ScienceDirect

Solid State Communications

journal homepage: http://www.elsevier.com/locate/ssc

Communication

Strong pinning and slow flux creep relaxation in Co-doped $CaFe_2As_2$ single crystals

N. Haberkorn [a,*], S. Suárez [a], S.L. Bud'ko [b,c], P.C. Canfield [b,c]

[a] Centro Atómico Bariloche and Instituto Balseiro, Universidad Nacional de Cuyo, CNEA and Consejo de Investigaciones Científicas y Técnicas Av. E. Bustillo 9500, R8402AGP, S. C. Bariloche, RN, Argentina
[b] Ames Laboratory, US DOE, Iowa State University, Ames, IA 50011, USA
[c] Department of Physics and Astronomy, Iowa State University, Ames, IA 50011, USA

ARTICLE INFO

Communicated by F. Peeters

Keywords:
A. Iron based superconductors
B. Single crystals
D. Vortex dynamics
E. Magnetization

ABSTRACT

We report on measurements of critical current densities J_c and flux creep rates S of freestanding $Ca(Fe_{1-x}Co_x)_2As_2$ ($x \approx 0.033$) single crystals with $T_c \approx 15.7$ K by performing magnetization measurements. The magnetic field dependences of J_c at low temperature display features related to strong pinning. In addition, we find that the system displays small flux creep rates. The characteristic glassy exponent, μ, and the pinning energy, U_0, display exceptional high values for pristine crystals. We find that for magnetic fields between 0.3 T and 1 T, μ decreases from ≈ 2.8 to ≈ 2 and U_0 remains ≈ 300 K. Analysis of the pinning force indicates that the mechanism is similar to the observed in polycrystalline systems in which grain boundaries and random disorder produce the vortex pinning. Considering the large U_0 observed in the single crystal, we attempt to improve the pinning by adding random point disorder by 3 MeV proton irradiation with a fluence of 2×10^{16} proton/cm^2. The results show that, unlike other iron-based superconductors, the superconducting fraction is sharply reduced by irradiation. This fact indicates that the superconductivity in the system is extremely fragile to an increment in the disorder. The superconducting volume fraction in the irradiated crystal systematically recovers after removal disorder by thermal annealing, which evidences as to the observation of critical state in curves of magnetization versus magnetic field. No features related to a reentrant antiferromagnetic transition are observed for the irradiated sample.

1. Introduction

The $Ca(Fe_{1-x}Co_x)_2As_2$ system displays three ground states (antiferromagnetic/orthorhombic, superconducting, and nonmagnetic/collapsed tetragonal) competing at low temperature, which can be modified using external control parameters such as chemical substitution, synthesis process or pressure [1–4]. Unlike electron doped $BaFe_2As_2$ [5], $Ca(Fe_{1-x}Co_x)_2As_2$ does not display coexistence of superconductivity (SC) with antiferromagnetic/orthorhombic phase [4]. SC emerges as structural transitions are suppressed by internal strain produced by FeAs nanoscale precipitation [3,4]. The highest superconducting critical temperature (T_c) for $Ca(Fe_{1-x}Co_x)_2As_2$ is ≈ 16 K with $x \approx 0.033$. Below $x \approx 0.028$, the samples do not show significant diamagnetism, indicating filamentary superconductivity. In overdoped samples T_c decreases gradually with increasing Co concentration and drops to around 2.5 K for $x = 0.059$ [4]. Biaxial strain induces alternating tetragonal superconducting and orthorhombic domains [6,7]. Moreover, T_c changes abruptly with hydrostatic pressure as $dT_c/dP \approx -60$ K/GPa [8].

The remarkable sensitivity of superconducting, magnetic, and structural properties to applied pressure or internal strain in $Ca(Fe_{1-x}Co_x)_2As_2$ single crystals makes them excellent candidates for basic and applied research. It was predicted that vortex core inducing stress could produce a peak in the reversible magnetization and that the inter-vortex interactions due to strain can produce a triangular to square vortex transition [9,10]. In addition, the extreme sensitivity of the phase separation to biaxial strain makes this system interesting for the design of Josephson junction networks [6]. Furthermore, by incorporating non-superconducting nano-inclusions in a reversible and controlled way, it is possible to modify the pinning strength, the dynamics and the configuration of the vortex lattice [11–16].

Here, we study the magnetic fields (H) and temperature (T)

* Corresponding author.
E-mail address: nhaberk@cab.cnea.gov.ar (N. Haberkorn).

https://doi.org/10.1016/j.ssc.2020.113963
Received 14 April 2020; Received in revised form 18 May 2020; Accepted 20 May 2020
Available online 26 May 2020

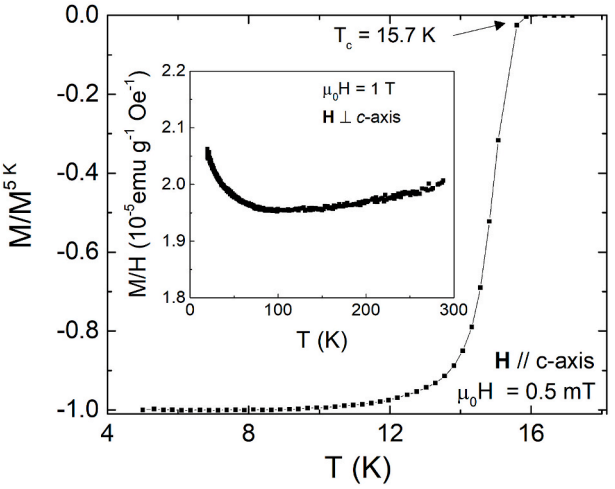

Fig. 1. Temperature dependence of the normalized magnetization (M/M^{5K}) with $\mu_0H = 0.5$ mT applied parallel to the *c*-axis in a $Ca(Fe_{1-x}Co_x)_2As_2$ (x = 0.033) single crystal. Inset shows the temperature dependence of the magnetic susceptibility with a magnetic field of 1 T applied perpendicular to the *c*-axis.

dependence of the J_c and flux creep rates S in a freestanding $Ca(Fe_{1-x}Co_x)_2As_2$ (x ≈ 0.033) single crystal by performing magnetization measurements. It is expected that the internal strain produced by nanoscale precipitates interacts with the stress generated by vortex cores [4,9]. Considering that ion irradiation is a well-established method for artificially introducing crystalline defects and enhancing the J_c values [17–19], the properties of pristine crystals are compared with those observed in the same crystal irradiated with 3 MeV protons (p) with a fluence of 2×10^{16} p/cm^2. Vortex dynamics is analyzed in the framework of the collective creep theory [20]. Characteristic glassy exponents μ and pinning energies U_0 are obtained from the extended Maley method [21,22]. Absolute J_c and S values are compared with single crystals of other iron based superconductors (Fe-SCs). The influence of the irradiation on the superconducting properties is discussed.

2. Experimental details

The single crystals of $Ca(Fe_{1-x}Co_x)_2As_2$ were grown according to the description provided in Ref. [4]. The studied crystals correspond to the composition x = 0.033. To minimize internal strain and obtain bulk superconductivity, the single crystals were annealed for 24 h at 400 °C [4]. As described in Refs. [3], this is most likely leads to the formation of meso-scaled FeAs inclusion in the otherwise single crystalline sample. The single crystals with bulk superconductivity obtained after annealing are denominated pristine in section 3.1. The magnetization measurements were performed using a superconducting quantum interference device (SQUID) magnetometer (Quantum Design MPMS). For J_c and S measurements, the magnetic field (**H**) was applied parallel to the *c* axis of the single crystal (**H**//*c*) with dimensions: 1.5 mm (length: l) x 1.2 mm (width: *w*) and 0.12 mm (thickness: *t*). The J_c values were calculated from the magnetization data using the appropriate geometrical factor in the Bean Model [23]. For **H**||*c*, $J_c = \frac{20\Delta M}{w(1-w/3l)}$, where ΔM (emu/cm^3) is the difference in magnetization between the top and bottom branches of the hysteresis loop. Magnetic relaxation measurements were recorded over periods of 1 h. The initial time for flux creep rates, $S = -\delta lnJ/dlnt$, was adjusted considering the best correlation factor in the log-log fitting of the $J(t)$ dependence. It is important to mention that the magnetic measurements at low temperatures after warming up to room temperature are reproducible. For comparison, the single crystal was irradiated with 3 MeV protons (p) with a fluence of 2×10^{16} p/cm^2. We choose this dose by considering that it produces a strong improvement in the vortex pinning of most Fe-SCs [24,25]. Considering the thickness and the ion

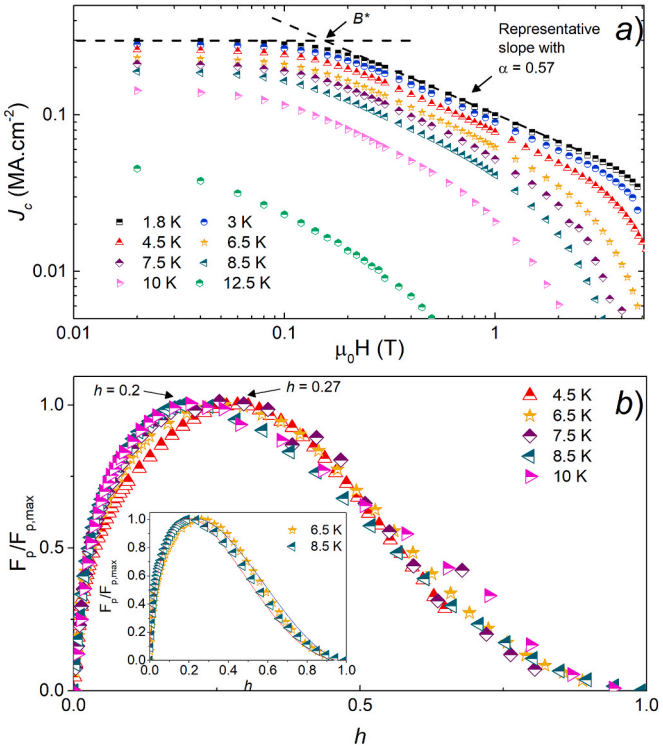

Fig. 2. a) Magnetic field dependence of the critical current density J_c in a Co-doped $CaFe_2As_2$ single crystal at different temperatures. b) Normalized pinning force ($F_P/F_{P,max}$) versus normalized magnetic field (h = h/h$_{irr}$(T) at different temperatures. Inset shows the curves for T = 6.5 K and 8.5 K and the respective fits using equation (1). The measurements where preformed with **H**//c-axis.

penetration in the material estimated from SRIM [26], two successive irradiation (one for each surface of the crystal) were performed. For comparison, the irradiated single crystal was successively annealed in vacuum (≈1×10^{-6} Torr) at 200 °C, 300 °C and 400 °C for 2 h.

3. Results and discussion

3.1. Pristine crystals

The T_c value in the $Ca(Fe_{1-x}Co_x)_2As_2$ (x = 0.033) single crystal obtained from a magnetization versus temperature measurement is 15.7 K (see Fig. 1). The superconducting properties for 0 ≤ x ≤ 0.058 were reported in Ref. [4]. The upper critical field $H_{c2}^{\|c}$ for x = 0.033 is ≈ 20 T with a Ginzburg-Landau coherence length $\xi_{GL}(0) = 5$ nm. The anisotropy parameter obtained from upper critical fields $\gamma = H_{c2}^{ab}/H_{c2}^{c}$ changes with temperature being ≈ 1.6 at 10 K and 2 near T_c [4]. The inset of Fig. 1 shows the temperature dependence of the magnetic susceptibility with $\mu_0H = 1$ T applied perpendicular to the *c*-axis. The curve does not display any jump or anomaly, consistent with earlier work [4] that showed that the magnetic/structural transition is fully suppressed.

Fig. 2*a* shows J_c (H) dependences for temperatures between 1.8 K and 12.5 K. The data are plotted on logarithmic scale. The self-field $J_c^{sf}(1.8\,K)$ is ≈ 0.3 MA cm^{-2} decreasing gradually as temperature increases. The value of $J_c^{sf}(1.8\,K)$ is similar to that previously observed in other Fe-SCs such as $Ba(Fe_{0.88}Co_{0.12})_2As_2$ with T_c ≈ 20 K [27], $Ca_{0.5}Na_{0.5}Fe_2As_2$ with T_c ≈ 16 K [28], $FeTe_{0.6}Se_{0.4}$ with T_c = 14.5 K [29], among others. However, in comparison with these systems, there is a notable difference related to the J_c (H) dependences. This fact may be related with a significant structural disorder due to the presence of FeAs precipitates discussed in Ref. [3,4]. Whereas most as-grown Fe-SCs display a second peak in the magnetization (SPM) associated with weak

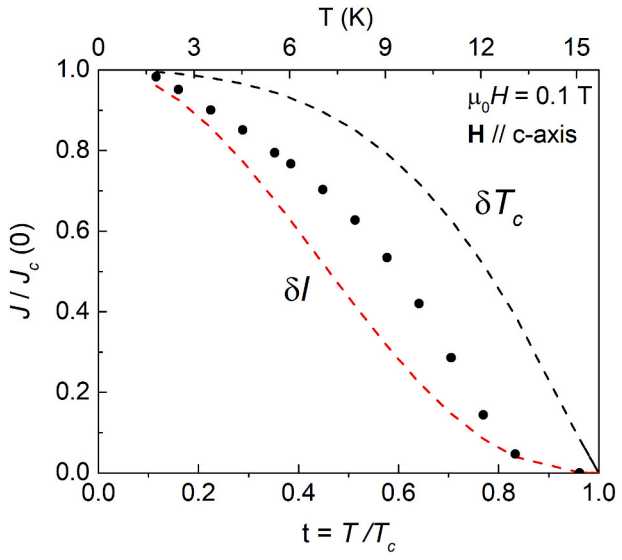

Fig. 3. Reduced temperature (T/T_c) dependence of J_c/J_c (0) experimental, and determined by δT_c and δl mechanism in a Co-doped $CaFe_2As_2$ single crystal. The measurement was performed with $\mu_0 H = 0.1$ T applied parallel to the c-axis.

pinning, the curves presented in Fig. 2*a* are characteristic of strong pinning [30]. At low fields, J_c is nearly constant up to a characteristic crossover field B^*, followed by a power-law regime ($J_c \propto H^{-\alpha}$) at intermediate fields, observed as a linear dependence on the log-log plot. Finally, at the higher fields, J_c decays quickly as H approaches to the irreversibility line H_{irr}. The crossover at B^* is usually defined as the step from single vortex to interactive vortices. The α value of spherical inclusions is predicted to be ≈ 1/2–5/8 [30]. The experimental value in Fig. 2*a* corresponds to α ≈ 0.58. Using the same criteria that for B^*, the crossover from the power-law regime to the high field regime with a fast drop of J_c at $T = 1.8$ K takes place at $\mu_0 H > 5$ T (≈ 0.25 H_{irr}). As the temperature increases, the crossover field B^* and the end of the power-law regime shift to lower fields.

The pinning mechanism in conventional superconductors can be analyzed by the scaling of the pinning force ($F_P = J_c \times H$). The F_p (*H, T*) can be scaled as

$$F_P \,/\, F_{P,\max} = A h^m (1-h)^l, \tag{1}$$

where $F_{p,max}$ is the maximum $F_p(H)$ at each temperature [31], A is a constant, m and l are exponents that depend on the pinning mechanism, and $h = H/H_{c2}$ (*T*). For Fe-SCs, we can replace H_{c2} by H_{irr}. We estimate the H_{irr} as the extrapolation to zero in a $J_c^{1/2} \times \boldsymbol{H}^{1/4}$ versus H plot [32]. This procedure has been successfully used in the case of wires, polycrystalline samples, and crystals [33–35]. Figure 2b shows $F_P/F_{P,\max}$ versus h for 4.5 K ≤ T ≤ 10.5 K. The results show two types of curves with the maximum at $h \approx 0.2$ (T > 8.5 K) and $h \approx 0.3$ (T < 7.5 K), indicating a change in the pinning mechanism. The former is similar to that observed in systems with vortex pinning provided by grain boundaries [36,37]. The later cannot be associated with a unique mechanism. Correspondingly, the theoretical F_p vs h curves present a maximum at different h values, the maximum is expected at $h = 0.33$ ($p = 1$, $q = 2$) for point defects and at $h = 0.2$ ($p = 1/2$, $q = 2$) for surface pinning centers, such as grain boundaries. On the other hand, strong pinning by normal inclusion usually shifts the maximum to $h > 0.33$ [31, 37]. Inset Fig. 2b shows the fits using equation (1) for 6.5 K and 8.5 K. The exponent are $m = 0.6$ and $l = 2.25$ for 6.5 K, and $m = 0.57$ and $l = 2.14$ for 8.5 K. It is noteworthy that the exponents obtained for both temperatures exhibit deviations from the theoretical predicted for a unique pinning source. There are a number of defect types that can act as pinning centers in $Ca(Fe_{1-x}Co_x)_2As_2$ (x ≈ 0.033) single crystals. In

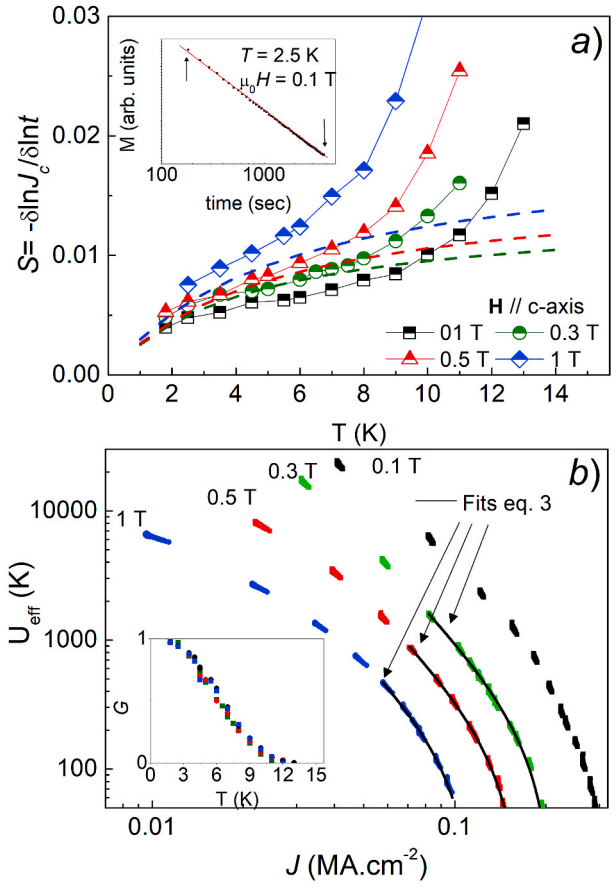

Fig. 4. *a)* Temperature dependence of the flux creep rates S with $\mu_0 H = 0.1$ T, 0.3 T. 0.5 T and 1 T. The measurements were performed with the magnetic field applied parallel to the *c*-axis. Dashed lines corresponds to the estimated values using equation (2) with ln (t/t_0) = 26 [42]. Inset shows typical curve of magnetization as function of time on a log-log scale. The slope corresponds to the S value. *b)* Maley analysis of the data presented in panel (a). Inset shows the *G* (T) function used to normalize the data.

particular, precipitates and dislocations [3,4]. On the other hand, random disorder also contributes to the pinning as is evidenced from a distorted hexagonal-like vortex lattice [6]. The presence of chemical inhomogeneities can be inferred from multiple step resistivity transitions for 16 K < T < 30 K [4]. The basic idea of pinning suggests that there is high competition between the energy scales of the different types of defects, but not all have the same contribution as the temperature increases. The scaling of the pinning force with $h_{max} \leq 0.3$ suggests that dislocations and strained regions are the main source of strong pinning in the crystals. It is important to note that most Fe-SCs display $h_{max} > 0.32$ [37].

The type of pinning in the superconductors can be understood as a result of spatial variations in T_c and in the electronic mean free path l (δT_c and δl pinning, respectively). Pinning by extended defects such as random nanoparticles corresponds to δT_c, while δl pinning applies to point defects. The respective functions for each mechanism in the single vortex regime as function of $t = T/T_c$ are $J_c\,(t)/J_c(0) = (1-t^2)^{7/6}(1+t^2)^{5/6}$ and $J_c\,(t)/J_c\,(0) = (1-t^2)^{5/2}(1+t^2)^{-1/2}$, respectively [38]. Fig. 3 shows a comparison between the theoretical predictions and the experimental data with $\mu_0 H = 0.1$ T applied parallel to the *c*-axis. The result reveals that the data is in the middle of both mechanisms. At low temperature (<12 K) the curvature is similar to that expected from δT_c, while near T_c decay as δl. In addition to a change in the pinning mechanism, the fast drop in the curve at ≈ 13 K could also be related to a diminution of the superconductor volume.

To understand why pinning in the crystals is strong, we performed

magnetic relaxation measurements at $\mu_0H = 0.1$ T, 0.3 T, 0.5 T, and 1 T. It is important to note that $\mu_0H = 0.1$ T is mostly below B^* (affected by self-field). The collective pinning theory predicts:

$$S = -\frac{\delta ln\, J}{\delta ln\, t} = \frac{T}{U_0 + \mu T ln\left(\frac{t}{t_0}\right)}, \quad (2)$$

with U_o the collective pinning barrier and t_0 a characteristic hopping time. Based on the model of the nucleation of vortex loops, for random point defects in the three-dimensional case, μ is 1/7, 3/2–5/2, and 7/9 for single vortex, small-bundle and large-bundle creep, respectively [20]. Systems with strong pinning usually present values in the range predicted for the collective creep theory for small bundles. For example, $YBa_2Cu_3O_{7-d}$ tapes display μ ≈ 1.7 [39]. Fig. 4*a* shows S (T) for the different applied fields. Inset Fig. 4a shows a typical $J(t)$ dependence in log-log scale. Unlike single crystals of most Fe-SCs with low U_0 and typical S values between 0.02 and 0.05 [24,25,27,29], the $S(T)$ dependences at low temperatures display an Anderson-Kim like dependence with $S \approx T/U_0$ starting from $S \approx 0.005$ at 1.8 K. As the temperature increases, the second term of the denominator in equation (2) contributes as is evidenced by the curvature. Finally, at high temperatures, the creep starts to be faster as a consequence of an increment in the thermal fluctuations and plastic relaxation [20,40]. High U_0 and low flux creep rates are usually observed in irradiated Fe-SCs single crystals [17,18,41]. To obtain the values of μ and U_0, we use the Maley analysis [21]. According to the collective creep theory, the dynamics in a glassy vortex phase is described by the effective activation energy U_{eff} as a function of current density (J):

$$U_{eff} = \frac{U_0}{\mu}\left[\left(\frac{J_c}{J}\right)^{\mu} - 1\right], \quad (3)$$

where $U_0\,(T) = U_0\,G(T)$ is the scale of the pinning energy and $G(T)$ and J_0 is the current density scale for the particular depinning process [22]. Approximating the current density decays as $\frac{dJ}{dt} = -\left(\frac{J_c}{\tau}\right)e^{-\frac{U_{eff}(J)}{T}}$, the effective activation energy $U_{eff}(J)$ can be experimentally obtained by $U_{eff} = -T\left[ln\left|\frac{dJ}{dt}\right| - C\right]$ (with $C = ln(J_c/\tau)$ a constant factor). To maintain "piecewise" continuity at high T, U_{eff} is divided by a thermal factor G(T) ≤ 1 [22]. Fig. 4*b* shows the Maley analysis for the data displayed in panel (a). Inset Fig. 4*b* shows the G(T) function used to give continuity to the pinning energy. We fit the data for $\mu_0H = 0.3$ T, 0.5 T and 1 T, for the range of temperature that corresponds to the power-law regime were fitted using equation (3). One of the issues related to the fits is that the obtained values for μ and U_0 strongly depend on the J_0. We correlate the J_0 values for the different fields using a $J_c \approx H^{-\alpha}$ dependence with α (1.8 K) = 0.58. For $\mu_0H = 0.3$ T, using $J_0 = 0.223$ (0.003) MA.cm^{-2}, we obtain μ = 2.80 (0.08) and $U_0 = 320$ (20) K. For $\mu_0H = 0.5$ T, using $J_0 = 0.167$ ((0.003) MA.cm^{-2}, we obtain μ = 2.40 (0.10) and $U_0 = 320$ (20) K. Finally, for $\mu_0H = 1$ T using $J_0 = 0.118$ (0.002) MA.cm^{-2}, we obtain μ = 2.05 (0.10) and $U_0 = 285$ (15) K. This analysis indicates the changes in $S(T)$ at different magnetic fields are mainly originated by a reduction in μ. We will now compare the experimental S (T) values with the predicted by equation (2) using the sets of (μ, U_0) and ln (t/t_0) ≈ 26 [42]. We find that the S (T) data for $\mu_0H = 0.3$ T and 0.5 T are quantitatively reproduced (see dashed lines in Fig. 4*a*), whereas lower S values are predicted for $\mu_0H = 1$ T. The glassy exponent μ = 2.5 corresponds to the prediction for elastic relaxation for small vortex bundles in a weak pinning scenario [20]. Similar μ values and gradual reduction as the magnetic field increases were previously reported in $Ba_{0.6}K_{0.4}BiO_3$ [43,44]. In our case, the large μ value obtained for 0.3 T may be related with pinning produced by a mixed pinning landscape and cannot be related to unique pinning mechanism. The strong pinning is evidenced in $U_0 \approx 300$ K, which is a value much higher than the usually observed in pristine

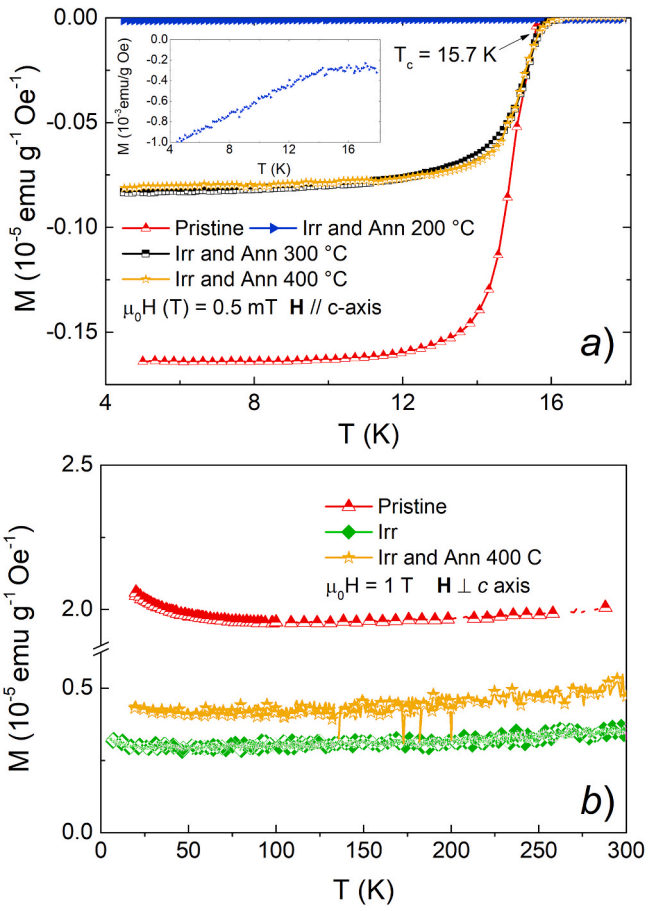

Fig. 5. *a)* Temperature dependence of the magnetic susceptibility with μ_0H = 0.5 mT applied parallel to the *c*-axis in a $Ca(Fe_{1-x}Co_x)_2As_2$ (x = 0.033) single crystal: pristine (before irradiation) and the irradiated crystal after thermal annealing at 200 °C, 300 °C and 400 °C. *b)* Temperature dependence of the magnetic susceptibility with $\mu_0H = 1$ T applied perpendicular to the *c*-axis in a $Ca(Fe_{1-x}Co_x)_2As_2$ (x = 0.033) single crystal: pristine (before irradiation), and the irradiated crystal before and after thermal annealing at 400 °C.

Fe-SCs single crystals [25,27,29,41]. Indeed, large U_0 and small flux creep rates are usually induced by proton and heavy ion irradiation [18].

The strength of the pinning potential usually is related to the $J_c./J_0$ ratio (here J_0 is the depairing critical current density). For low-T_c superconductors, pinning is usually strong ($J_c/J_0 \sim 10^{-2}$–10^{-1}) resulting from the interaction of vortices with extended defects, such as precipitates or grain boundaries. On the contrary, for the cuprate family, pinning is usually weak ($J_c/J_0 \sim 10^{-3}$–10^{-2}) normally arising from point defects. For $Ca(Fe_{1-x}Co_x)_2As_2$ (x ≈ 0.033) single crystals, assuming λ (0) ≈ 450 nm [45] and ξ (0) = 5 nm [4] and $J_0 \approx 9$ MA cm^{-2} and J_c (1.8 K) ≈ 0.3 MA cm^{-2}, we obtain $J_c/J_0 \approx 0.03$. The most likely scenario for the pinning in the freestanding $Ca(Fe_{1-x}Co_x)_2As_2$ (x ≈ 0.033) single crystals includes normal inclusions, domain boundaries, and random disorder. In addition, defects such as dislocations are originated from the thermal quench and are located at the interface between normal precipitates and the superconducting matrix. In contrast to other Fe-SCs such as CaKFe$_4$As$_4$ with $\xi_{GL}(0) \approx 1.4$ nm [46], the relative large $\xi_{GL} \approx 5$ nm reduces the contribution of random disorder to the pinning. Indeed, the vortex lattice exhibits a hexagonal-like array instead of a disordered lattice produced by random disorder [6,46].

3.2. Irradiated crystals

To understand more in-depth the nature of this strong pinning in these crystals, we performed irradiation using 3 MeV proton with a

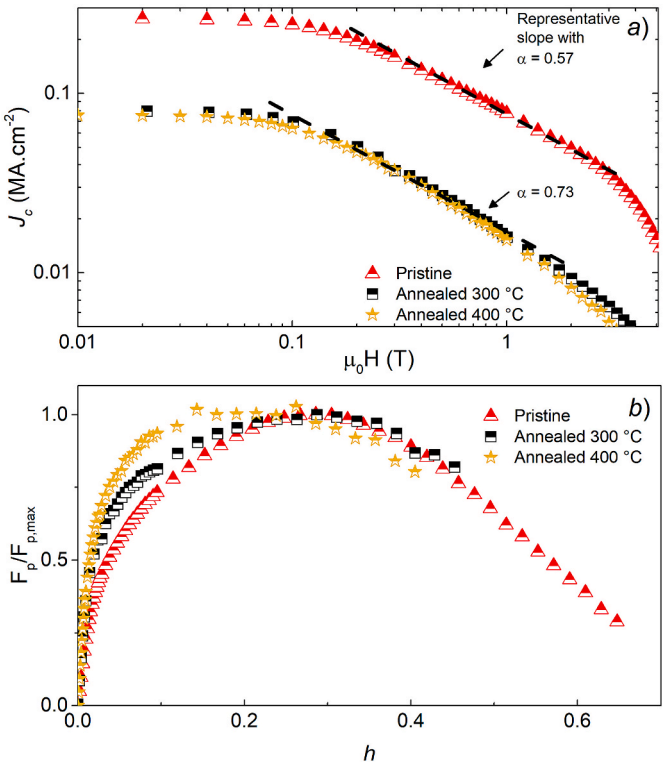

Fig. 6. a) Comparison between the magnetic field dependence of the critical current density J_c at 4.5 K in a Co-doped $CaFe_2As_2$ single crystal before irradiation and after be irradiated and annealed at 300 °C and 400 °C. b) Normalized pinning force ($F_P/F_{P,max}$) versus normalized magnetic field (h = h/h_{irr}(T)) for the curves displayed in a). The measurements where preformed with **H**//c-axis.

fluence of 2×10^{16} p/cm^2. Fig. 5a shows a comparison of the magnetic susceptibility with μ_0H = 0.5 mT applied parallel to the *c*-axis (after zero-field cooling) for the pristine crystal and the irradiated crystal after annealing at different temperatures. The irradiated crystal (not included) does not display a diamagnetic signal, indicating that, unlike other Fe-SCs such as FeSe and $Ca_{1-x}Na_xFe_2As_2$ [24,25], the superconducting state is exceptionally fragile. Indeed, filamentary superconductivity emerges after annealing at 200 °C (see inset Fig. 5a). Thermal annealing at higher temperatures (300 °C and 400 °C) increases the superconducting volume as evidence in a narrow transition (similar to before irradiation) and in the increase of the magnetic signal. Like in pristine single crystals, it is expected that the superconductor volume for irradiated crystal fully recovers by optimizing the annealing process [4]. The significant reduction of the superconductor volume produced by the irradiation suggests that random disorder may act locally in a similar way that biaxial strain [7].

Another feature to analyze in the irradiated samples is the presence of reentrant structural transitions. It is important to note that initially superconductivity emerges by suppressing structural phase transitions [4]. Fig. 5*b* shows a comparison of the temperature dependence of the magnetic susceptibility with μ_0H = 1 T applied perpendicular to the *c*-axis for the crystal before and after irradiation, and for the irradiated crystal after annealing at 400 °C. The results show that the disorder decreases the magnetic susceptibility. No features related to structural/magnetic transitions are observed.

Fig. 6a shows J_c (*H*) dependences at 4.5 K for the pristine and the irradiated crystal after thermal annealing. The results show that although thermal annealing increases the superconductor volume, the J_c values at low fields for the annealed samples are approximately 1/3 of those observed before irradiation. This fact may be related to a no fully recover of the superconductor volume with the performed thermal annealing, which is consistent with the lower diamagnetic signal observed in Fig. 5a. Fig. 6*b* shows $F_P/F_{p.max}$ versus *h* for 4.5 K for the curves displayed in panel a). The scaling of the pinning forces for the annealed samples display a broad peak with higher contributions at $h \approx 0.2$, which may be related to significant pinning by strained regions or domain boundaries due to a reduced superconducting volume.

4. Conclusions

In summary, we report on measurements of critical current densities J_c and flux creep rates *S* of free-standing $Ca(Fe_{1-x}Co_x)_2As_2$ ($x \approx 0.033$) single crystals with $T_c \approx 15.7$ K by performing magnetization measurements. The structural disorder in the crystals produces strong pinning reducing the flux creep rates as a consequence of large U_0. The strong pinning may be related to normal inclusions produced due to a minority of FeAs precipitates, dislocations, and strained regions due to variations in the chemical composition. Moreover, the scaling of the pinning forces displays similitude with polycrystalline systems. Finally, it is important to note that there are not apparent features in our study that may be directly related to vortex cores inducing stress [9], which may be related with the complex microstructure and the strong pinning displayed by the single crystals. For comparison, the sample was irradiated with 3 MeV protons at a fluence of 2×10^{16} p/cm^2. The irradiation reduces the superconducting volume indicating that the state is extremely fragile. Although superconductivity is suppressed, no features related to reentrant structural/magnetic transitions are observed.

Declaration of competing interest

The authors declare that there is no conflict of interest.

Acknowledgments

We would like to acknowledge S. Ran for sample preparation. The samples used correspond to a part of work presented in Refs. [4]. This work was supported by the U.S. Department of Energy, Office of Basic Energy Science, Division of Materials Sciences and Engineering. The research was performed at the Ames Laboratory. Ames Laboratory is operated for the U.S. Department of Energy by Iowa State University under Contract No. DE-AC02-07CH11358. N. H. and S. S. are partially supported by PICT 2015–2171 (Argentina).

References

[1] L. Harnagea, S. Singh, G. Friemel, N. Leps, D. Bombor, M. Abdel-Hafiez, A.U. B. Wolter, C. Hess, R. Klingeler, B. Behr, S. Wurmehl, B. Büchner, Phys. Rev. B 83 (2011), 094523, https://doi.org/10.1103/PhysRevB.83.094523.
[2] Marcin Matusiak, Zbigniew Bukowski, Janusz Karpinski, Phys. Rev. B 81 (2010), https://doi.org/10.1103/PhysRevB.81.020510, 020510(R).
[3] S. Ran, S.L. Bud'ko, D.K. Pratt, A. Kreyssig, M.G. Kim, M.J. Kramer, D.H. Ryan, W. N. Rowan- Weetaluktuk, Y. Furukawa, B. Roy, A.I. Goldman, P.C. Canfield, Phys. Rev B 83 (2011), 144517, https://doi.org/10.1103/PhysRevB.83.144517.
[4] S. Ran, S.L. Bud'ko, W.E. Straszheim, J. Soh, M.G. Kim, A. Kreyssig, A.I. Goldman, P.C. Canfield, Phys. Rev B 85 (2012), 224528, https://doi.org/10.1103/PhysRevB.85.224528.
[5] P.C. Canfield, S.L. Bud'ko, Ni Ni, J.Q. Yan, A. Kracher, Phys. Rev B 80 (2009), https://doi.org/10.1103/PhysRevB.80.060501, 060501(R).
[6] Antón Fente, Alexandre Correa-Orellana, Anna E. Böhmer, Andreas Kreyssig, S. Ran, Sergey L. Bud'ko, Paul C. Canfield, Federico J. Mompean, Mar García-Hernández, Carmen Munuera, Isabel Guillamón, Hermann Suderow, Phys. Rev B 97 (2018), 014505, https://doi.org/10.1103/PhysRevB.97.014505.
[7] A. E. Böhmer, A. Sapkota, A. Kreyssig, S. L. Bud'ko, G. Drachuck, S. M. Saunders, A. I. Goldman, P. C. Canfield, Phys. Rev. Lett. 118 (2017), 107002, https://doi.org/10.1103/PhysRevLett.118.107002.
[8] E. Gati, S. Köhler, D. Guterding, B. Wolf, S. Knöner, S. Ran, S.L. Bud'ko, P. C. Canfield, M. Lang, Phys. Rev B 86 (2012), 220511, https://doi.org/10.1103/PhysRevB.86.220511.
[9] V.G. Kogan, Phys. Rev B 87 (2014), https://doi.org/10.1103/PhysRevB.87.020503, 020503 (R).
[10] Shi-Zeng Lin, G. Vladimir, Kogan Phys. Rev B 95 (2017), 054511, https://doi.org/10.1103/PhysRevB.95.054511.

[11] L. Fang, Y. Jia, C. Chaparro, G. Sheet, H. Claus, M.A. Kirk, A.E. Koshelev, U. Welp, G.W. Crabtree, W.K. Kwok, S. Zhu, H.F. Hu, J.M. Zuo, H.-H. Wen, B. Shen, Appl. Phys. Lett 101 (2012), 012601, https://doi.org/10.1063/1.4731204.
[12] Masashi Miura, Boris Maiorov, Takeharu Kato, Takashi Shimode, Keisuke Wada, Seiji Adachi, Keiichi Tanabe, Nature Comm 4 (2013) 2499, https://doi.org/10.1038/ncomms3499.
[13] L. Embon, Y. Anahory, A. Suhov, D. Halbertal, J. Cuppens, A. Yakovenko, A. Uri, Y. Myasoedov, M.L. Rappaport, M.E. Huber, A. Gurevich, E. Zeldov, Scientific Reports 5 (2015) 7598, https://doi.org/10.1038/srep07598.
[14] L. Embon, Y. Anahory, Ž.L. Jelić, E.O. Lachman, Y. Myasoedov, M.E. Huber, G. P. Mikitik, A.V. Silhanek, M.V. Milošević, A. Gurevich, E. Zeldov, Nature Comm 8 (2017) 85, https://doi.org/10.1038/s41467-017-00089-3.
[15] José Benito Llorens, et al., Phys. Rev. Research 2 (2020), 013329, https://doi.org/10.1103/PhysRevResearch.2.013329.
[16] N. Haberkorn, H. Troiani, A.M. Condó, Hangdong Wang, Qianhui Mao, Minghu Fang, Solid Sta. Comm. 247 (2016) 88–93, https://doi.org/10.1016/j.ssc.2016.08.022.
[17] Tsuyoshi Tamegai, Toshihiro Taen, Hidenori Yagyuda, Yuji Tsuchiya, Shyam Mohan, Tomotaka Taniguchi, Yasuyuki Nakajima, Satoru Okayasu, Masato Sasase, Hisashi Kitamura, Supercond. Sci. Technol. 25 (2012), 084008, https://doi.org/10.1088/0953-2048/25/8/084008.
[18] Wai-Kwong Kwok, Welp Ulrich, Andreas Glatz, Alexei E. Koshelev, Karen J. Kihlstrom, George W. Crabtree, Rep. Prog. Phys. 79 (2016), 116501, https://doi.org/10.1088/0034-4885/79/11/116501.
[19] M. Eisterer, Supercond. Sci. Technol. 31 (2018), 013001, https://doi.org/10.1088/1361-6668/aa9882.
[20] G. Blatter, M.V. Feigel'man, V.B. Geshkenbein, A.I. Larkin, V.M. Vinokur, Rev. Mod. Phys. 66 (1994) 1125, https://doi.org/10.1103/RevModPhys.66.1125.
[21] M.P. Maley, J.O. Willis, H. Lessure, M.E. McHenry, Phys. Rev. B 42 (1990) 2639, https://doi.org/10.1103/PhysRevB.42.2639.
[22] J.G. Ossandon, J.R. Thompson, D.K. Christen, B.C. Sales, Yangren Sun, K.W. Lay, Phys. Rev. B 46 (1992) 3050, https://doi.org/10.1103/PhysRevB.46.3050.
[23] (a) C.P. Bean, Phys. Rev. Lett. 8 (1962) 250, https://doi.org/10.1103/PhysRevLett.8.250;
(b) C.P. Bean, Rev. Mod. Phys 36 (1964) 31, https://doi.org/10.1103/RevModPhys.36.31.
[24] M.L. Amigó, N. Haberkorn, P. Pérez, S. Suárez, G. Nieva, Supercond. Sci. Technol. 30 (2017), 125017. https://orcid.org/0000-0001-6977-271X.
[25] N. Haberkorn, Jeehoon Kim, B. Maiorov, I. Usov, G.F. Chen, W. Yu, L. Civale, Supercond. Sci. Technol. 27 (2014), 095004, https://doi.org/10.1088/0953-2048/27/9/095004.
[26] J.F. Ziegler, M.D. Ziegler, J.P. Biersack, in: 19th International Conference on Ion Beam Analysis Nuclear Instruments and Methods in Physics Research Section B: Beam Interactions with Materials and Atoms vol. 268, 2010, pp. 1818–1823.
[27] Bing Shen, Peng Cheng, Zhaosheng Wang, Lei Fang, Cong Ren, Lei Shan, Hai-Hu Wen, Phys. Rev B 81 (2010), 014503, https://doi.org/10.1103/PhysRevB.81.014503.
[28] N. Haberkorn, B. Maiorov, M. Jaime, I. Usov, M. Miura, G.F. Chen, W. Yu, L. Civale, Phys. Rev. B 84 (2011), 064533, https://doi.org/10.1103/PhysRevB.84.064533.
[29] Yue Sun, Toshihiro Taen, Yuji Tsuchiya, Sunseng Pyon, Zhixiang Shi, Tsuyoshi Tamegai EPL 103 (2013) 57013, https://doi.org/10.1209/0295-5075/103/57013.
[30] C.J. van der Beek, M. Konczykowski, A. Abal'oshev, I. Abal'osheva, P. Gierlowski, S.J. Lewandowski, M.V. Indenbom, S. Barbanera, Phys. Rev. B 66 (2002), 024523, https://doi.org/10.1103/PhysRevB.66.024523.
[31] D. Dew-Hughes, Phil. Mag. 30 (1974) 293, https://doi.org/10.1080/14786439808206556.
[32] J. Kramer Edward, J. Appl. Phys. 44 (1973) 1360, https://doi.org/10.1063/1.1662353.
[33] J.W. Ekin, Cryogenics 20 (1980) 611, https://doi.org/10.1016/0011-2275(80)90191-5.
[34] R. Flukiger, C. Senatore, M. Cesaretti, F. Buta, D. Uglietti, B. Seeber, Supercond. Sci. Technol. 21 (2008), 054015, https://doi.org/10.1088/0953-2048/21/5/054015.
[35] Marco Bonura, Enrico Giannini, Romain Viennois, Carmine Senatore, Phys. Rev B 85 (2012), 134532, https://doi.org/10.1103/PhysRevB.85.134532.
[36] T. Baumgartner, M. Eisterer, H.W. Weber, R. Flükiger, C. Scheuerlein, L. Bottura Supercond, Sci. Technol. 27 (2014), 015005, https://doi.org/10.1088/0953-2048/27/1/015005.
[37] M.R. Koblischka, M. Murakami, Inter. J. Modern Phys. B 30 (2016), 1630017, https://doi.org/10.1142/S0217979216300176.
[38] R. Griessen, W. Hai-hu, A.J.J. van Dalen, B. Dam, J. Rector, H.G. Schnack, S. Libbrecht, E. Osquiguil, Y. Bruynseraede, Phys. Rev. Lett. 72 (1994) 1910, https://doi.org/10.1103/PhysRevLett.72.1910.
[39] A.O. Ijaduola, S.H. Wee, A. Goya, P.M. Martin, J. Li, J.R. Thompson, D. K. Supercond, Sci. Technol. 25 (2012), 045013, https://doi.org/10.1088/0953-2048/25/4/045013.
[40] Y. Abulafia, A. Shaulov, Y. Wolfus, R. Prozorov, L. Burlachkov, Y. Yeshurun, D. Majer, E. Zeldov, H. Wüh, V.B. Geshkenbein, V.M. Vinokur, Phys. Rev Lett 77 (1996) 1596, https://doi.org/10.1103/PhysRevLett.77.1596.
[41] N. Haberkorn, Jeehoon Kim, K. Gofryk, F. Ronning, A.S. Sefat, L. Fang, U. Welp, W.-K. Kwok, L. Civale, Supercond. Sci. Technol. 28 (2015), 055011, https://doi.org/10.1088/0953-2048/28/5/055011.
[42] J.R. Thompson, L. Krusin-Elbaum, L. Civale, G. Blatter, C. Field, Phys. Rev Lett 78 (1997) 3181, https://doi.org/10.1103/PhysRevLett.78.3181.
[43] T. Klein, W. Harneit, I. Joumard, J. Marcus, C. Escribe-Filippini, D. Feinberg, Europhys. Lett. 42 (1998) 79, https://doi.org/10.1209/epl/i1998-00555-0.
[44] I. Joumard, T. Klein J. Marcus, Phys. Review Lett. 87 (2001), 167002, https://doi.org/10.1103/PhysRevLett.87.167002.
[45] Luan Lan, Thomas M. Lippman, Clifford W. Hicks, Julie A. Bert, Ophir M. Auslaender, Jiun-Haw Chu, James G. Analytis, Ian R. Fisher, Kathryn A. Moler, Phys. Rev Lett 106 (2011), 067001, https://doi.org/10.1103/PhysRevLett.106.067001.
[46] Antón Fente, William R. Meier, Tai Kong, Vladimir G. Kogan, Sergey L. Bud'ko, Paul C. Canfield, Isabel Guillamón, Hermann Suderow, Phys Rev B 97 (2018), 134501, https://doi.org/10.1103/PhysRevB.97.134501.